

Instabilities of variable-density swirling flows

Bastien Di Pierro and Malek Abid*

IRPHE-UMR 6594, Technopôle de Château-Gombert, 49 rue Joliot Curie, BP 146, 13384 Marseille Cedex 13, France

(Received 27 July 2010; published 26 October 2010)

Inviscid swirling flows are modeled, for analytical studies, using axisymmetric azimuthal, $V(r)$, and axial, $W(r)$, velocity profiles (r is the distance from the axis). The asymptotic analysis procedure (large wave numbers, k axial and m azimuthal) developed by Leibovich and Stewartson [*J. Fluid Mech.* **126**, 335 (1983)], and used by many authors, breaks down if $kW'(r)+m\Omega'(r)\neq 0, \forall r$ or if $kW'(r)+m\Omega'(r)=0, \forall r, \Omega=V/r$. This latter case occurs if W is constant with $m=0$, if Ω is constant with $k=0$, or if both W and Ω are constant with arbitrary wave-number vector. These particular cases are considered by Leblanc and LeDuc [*J. Fluid Mech.* **537**, 433 (2005)]. Thus, the case where W and Ω both vary and the Leibovich and Stewartson asymptotics breaks down remains. It is addressed in the present paper for weak variations of axial and azimuthal velocities. The asymptotic results are checked using numerically computed growth rates of the linearized Euler equations for a family of variable-density Batchelor-like vortices as base flows. Good agreement is found even for low values of m and k .

DOI: [10.1103/PhysRevE.82.046312](https://doi.org/10.1103/PhysRevE.82.046312)

PACS number(s): 47.20.Cq, 47.32.Ef

I. INTRODUCTION

Swirling flows are widely studied in the literature. The understanding of mechanisms of their stability (or instability) is of great importance in the design of control strategies for aircraft wakes and for many combustion devices. Furthermore, from a fundamental viewpoint, swirling flows are present in turbulent flows, and their breakdown is a possible mechanism for generating small scales in such flows [1–3]. It is out the scope of the present paper to summarize the vast swirling flow literature. However, the following papers are particularly enlightening for the purpose of the present study. Howard and Gupta [4] derived an equation for constant-density inviscid instability analysis. Later, Leibovich and Stewartson [5] used this equation, carried out asymptotical analysis (for large wave numbers), and are able to construct a discrete set of eigenmodes localized radially around the extremum of the Doppler frequency: $mV/r+kW-\omega$ (with ω being the eigenmode frequency). Using these eigenmodes, they derived a sufficient condition for swirling flow instability. Independently, with the aid of a generalized WKB method, Eckhoff and Storesletten [6] derived a sufficient condition for *compressible* swirling flow instability including the sufficient condition of Leibovich and Stewartson [5] as a particular case. Recently, using an original formalism, Leblanc and LeDuc [7] established a connection between the Eckhoff and Storesletten [6] spectrum (and called it the continuous spectrum) and the discrete spectrum of Leibovich and Stewartson [5]. Particularly they showed that the points of the continuous spectrum are accumulation points for the discrete spectrum.

The above cited studies break down if $kW'(r)+m\Omega'(r)\neq 0, \forall r$ or if $kW'(r)+m\Omega'(r)=0, \forall r, \Omega=V/r$ (where $'$ represents differentiation with respect to r). This latter case occurs if W is constant with $m=0$, if Ω is constant with $k=0$, or if both W and Ω are constant with arbitrary wave-number

vector. These particular cases are considered by Leblanc and LeDuc [7]. Thus, the case where W and Ω both vary and the Leibovich and Stewartson asymptotics breaks down remains. It is addressed in the present paper for weak variations of axial and azimuthal velocities, but with no restrictions on density variations.

II. DISTURBANCE EQUATION

In this section, we focus on the destabilization of an inviscid swirling flow with density variations. Thus, incompressible Euler equations linearized around the basic flow $\mathbf{U}(\mathbf{x})=[0, V(r), W(r)]_{(\mathbf{e}_r, \mathbf{e}_\theta, \mathbf{e}_z)}$ and density $\rho_b(r)$ are considered:

$$\frac{\partial \rho}{\partial t} + \mathbf{U} \cdot \nabla \rho + \mathbf{u} \cdot \nabla \rho_b = 0,$$

$$\frac{\partial \mathbf{u}}{\partial t} + \mathbf{U} \cdot \nabla \mathbf{u} + \mathbf{u} \cdot \nabla \mathbf{U} = -\frac{\nabla P}{\rho_b} + \frac{\rho}{\rho_b^2} \nabla P,$$

$$\nabla \cdot \mathbf{u} = 0, \quad (1)$$

with $\nabla P = (dP/dr)\mathbf{e}_r = \rho_b(V^2/r)\mathbf{e}_r$, and (\mathbf{u}, p, ρ) are, respectively, the perturbations of velocity, pressure, and density. Thanks to helical symmetry of the basic flow, the perturbations (in a cylindrical frame) are sought as

$$(u, v, w, p, \rho) = (iu(r), v(r), w(r), p(r), \rho(r)) \times \exp[i(-\omega t + m\theta + kz)], \quad (2)$$

in a classical linear temporal problem, where k is the (real) axial wave number, m is the azimuthal (integer) wave number, and ω is the complex unknown frequency. Vanishing of

*Corresponding author; abid@irphe.univ-mrs.fr

perturbations is required far from the flow axis. To shorten the notation, we introduce some new variables: $l=m/r$, $\Sigma=kW+lV-\omega$, $\Omega=V/r$, and $\Theta=V'+\Omega$.

After some algebra, the partial differential equation system (1) is rewritten as an ordinary differential one:

$$\rho_b \left[-\Sigma u + 2 \frac{V}{r} \left(\frac{l}{\rho_b \Sigma} p + \frac{\Theta}{\Sigma} u \right) \right] + \frac{V^2}{\Sigma r} \frac{d\rho_b}{dr} u = - \frac{dp}{dr}, \quad (3)$$

$$\frac{1}{r} \frac{dru}{dr} - \left(\frac{l^2 + k^2}{\rho_b \Sigma} \right) p - \left(\frac{l\Theta + kW'}{\Sigma} \right) u = 0. \quad (4)$$

Let the Rayleigh discriminant be $\Phi=r^{-3}d(r^2V^2)/dr=2\Omega\Theta$, G (the analog of the Brunt-Väisälä frequency) defined as $G^2=-(V^2/r)\rho'_b/\rho_b$, and H defined as $H^2=G^2-\Phi$. Then, the system of equations (3) and (4) can be reduced to the following second-order ordinary differential equation :

$$\underbrace{\frac{r(l^2+k^2)}{\rho_b} \frac{d}{dr} \left(\frac{\rho_b}{r(l^2+k^2)} \frac{d\psi}{dr} \right)}_I - \underbrace{\left[\frac{k}{\rho_b \Sigma} \frac{d\rho_b W'}{dr} + k^2 \left(1 + \frac{H^2}{\Sigma^2} \right) - \frac{W'}{\Sigma} \frac{k^3}{r(l^2+k^2)} \right]}_{II} \psi - \underbrace{\left[\frac{l}{\rho_b \Sigma} \frac{d\rho_b \Theta}{dr} + l^2 \left(1 + \frac{G^2}{\Sigma^2} \right) \right]}_{III} \psi + \underbrace{\left[\frac{1}{r(k^2+l^2)\Sigma} (2k^2 l \Theta - kl^2 W') - \frac{2VklW'}{r \Sigma^2} \right]}_{IV} \psi = 0, \quad (5)$$

with $\psi=ru$. This equation coupled with the boundary conditions $\psi(0)=\psi(\infty)=0$ forms a classical eigenvalue problem for the complex frequency ω .

An interesting feature of this equation is that the axial velocity W will not affect instabilities with $k=0$. Note that for no axial velocity, $W=0$, the main equation obtained in [8] is recovered, and in the constant-density case ($\rho_b=1$), this equation is equivalent to the one obtained by [4] for nonmagnetic fluid and nonaxisymmetric disturbances.

Writing Eq. (5) in this form will let us express the square of the leading part of the growth rate as a linear combination of those of two orthogonal eigenstates: ($m \neq 0, k=0$) and ($m=0, k \neq 0$). Effectively, term II vanishes for $k=0, m \neq 0$, term III vanishes for $k \neq 0, m=0$, whereas the last term IV is responsible for the three-dimensional destabilization due to the coupling between axial and azimuthal velocities. Note that this last term is nonzero only for three-dimensional nonaxisymmetric perturbations: $m \neq 0$ and $k \neq 0$.

Equation (5) contains a nontrivial differentiation term: term I. To simplify this equation, we introduce $\alpha=\rho_b/[r(l^2+k^2)]$ and $\beta=II+III+IV$. After the transform $\phi=\sqrt{\alpha}\psi$, Eq. (5) reads

$$\frac{d^2}{dr^2} \phi + \left[\left(\frac{\alpha'}{2\alpha} \right)^2 - \frac{\alpha''}{2\alpha} + \beta \right] \phi = 0. \quad (6)$$

III. ASYMPTOTICAL STUDY: THE GENERAL CASE

In this section, we focus on the asymptotical structure of Eq. (6), and high azimuthal and axial wave numbers are therefore considered: $|m| \gg 1, |k| \gg 1$. In order to construct rescaled wave numbers of order unity, a small parameter ε is introduced ($0 < \varepsilon \ll 1$), and we define

$$\tilde{m} = \varepsilon m, \quad \tilde{k} = \varepsilon k. \quad (7)$$

In Eq. (6), the terms α'/α and α''/α are both of order unity. Using the rescaled wave numbers above, introducing the new variable χ defined as

$$\chi^2 = \frac{m^2 G^2 + k^2 r^2 H^2 + 2mkr\Omega W'}{m^2 + k^2 r^2} = \frac{\tilde{m}^2 G^2 + \tilde{k}^2 r^2 H^2 + 2\tilde{m}\tilde{k}r\Omega W'}{\tilde{m}^2 + \tilde{k}^2 r^2}, \quad (8)$$

and after an expansion in powers of ε , Eq. (6) reads¹

$$\frac{d^2 \phi}{dr^2} - \varepsilon^{-2} \frac{\tilde{m}^2 + \tilde{k}^2 r^2}{r^2} \left[1 + \frac{\chi^2}{\Sigma^2} \right] \phi + O(\varepsilon^{-1}) = 0. \quad (9)$$

Following [7], in the limit $\varepsilon \rightarrow 0$, and if for some $r_0 > 0, \chi^2(r_0) = -\Sigma^2(r_0)$, the generalized solution is then $\phi(r) = \delta(r-r_0)$. Assuming that $\chi^2(r_0) > 0$, the eigensolution $\omega = \varepsilon^{-1}(m\Omega + kW) - \Sigma$ is then

$$\omega_0 = \varepsilon^{-1}(\tilde{m}\Omega_0 + \tilde{k}W_0) + i\chi_0, \quad (10)$$

with $\chi_0 = \sqrt{\chi^2(r_0)}$, and “0” subscripted functions are evaluated at $r=r_0$. However, this solution is valid in the singular limit $\varepsilon \rightarrow 0$ and is not square integrable. Thus, this solution is called “singular spectrum” (we prefer this designation over the term “continuous spectrum”).

¹Equation (3.4) of [7] is erroneous: for incompressible fluids, their Σ^2 must be replaced with our χ^2 . However, their conclusions are not affected since the modes are localized in the vicinity of the radius r where $m\Omega' + kW' = 0$.

In order to evaluate the eigensolution corresponding to smooth eigenfunctions, the following rescaled variables are used (assuming that Ω' and W' are small, but that Ω and W are of order unity in the vicinity of r_0):

$$\tilde{r} = \frac{r - r_0}{\varepsilon^{\alpha_1}}, \quad \tilde{\omega} = \frac{\omega - \omega_0}{\varepsilon^{\alpha_2}}, \quad \tilde{\Omega}(r) = \frac{\Omega(r) - \Omega_0}{\varepsilon^{\alpha_3}},$$

$$\tilde{W}(r) = \frac{W(r) - W_0}{\varepsilon^{\alpha_3}}, \quad (11)$$

and $\tilde{\phi}(\tilde{r}) = \phi(r)$, where $\alpha_1, \alpha_2, \alpha_3$ are positive parameters to be found; \tilde{r} is the rescaled, $O(1)$, radii; and $\tilde{\omega}$ is the complex frequency to be determined. For basic flows and densities that are *axisymmetric* and derivable at $r=0$ and are bounded in the limit $r \rightarrow \infty$, we have $\chi(0)=0$ and $\chi(r \rightarrow \infty)=0$. Therefore, the function χ is extremal somewhere in the flow. Let r_0 be the location of such an extremum: $\chi'_0 = \chi'(r_0)=0$. By studying the equation near r_0 , we obtain, at the *leading order*

$$\frac{d^2 \tilde{\phi}}{d\tilde{r}^2} + \varepsilon^{2\alpha_1 - 2} \frac{\tilde{m}^2 + \tilde{k}^2 r_0^2}{r_0^2 \chi_0} [2i(\tilde{\omega} \varepsilon^{\alpha_2} + \varepsilon \Gamma_0) + \tilde{r}^2 \varepsilon^{2\alpha_1} \chi_0'' - 2i\tilde{r} \varepsilon^{-1 + \alpha_1 + \alpha_3} (\tilde{m} \tilde{\Omega}'_0 + \tilde{k} \tilde{W}'_0)] \tilde{\phi} = 0, \quad (12)$$

$$\Gamma_0 = \frac{\tilde{m} \Omega_0}{\tilde{m}^2 + \tilde{k}^2 r_0^2} \left(\frac{2\tilde{k}^2 r_0^2}{\tilde{m}^2 + \tilde{k}^2 r_0^2} - r_0 \frac{\rho'_{b0}}{\rho_{b0}} \right). \quad (13)$$

All the terms of Eq. (13) are assumed to be, at least, of order unity. Therefore, the following scalings are found: $\alpha_1 = 1/2$, $\alpha_2 = 1$, and $\alpha_3 = 3/2$. Hence, the problem to solve is

$$\frac{d^2 \tilde{\phi}}{d\tilde{r}^2} + \frac{\tilde{m}^2 + \tilde{k}^2 r_0^2}{r_0^2 \chi_0} [2i(\tilde{\omega} + \Gamma_0) + \tilde{r}^2 \chi_0'' - 2i\tilde{r}(\tilde{m} \tilde{\Omega}'_0 + \tilde{k} \tilde{W}'_0)] \tilde{\phi} = 0, \quad (14)$$

which is a generalized parabolic cylinder differential equation. This equation is rewritten as a Weber equation by completing the square and using the following rescaling:

$$b = 2i \frac{(\tilde{m}^2 + r_0^2 \tilde{k}^2)}{r_0^2} \frac{(\tilde{m} \tilde{\Omega}'_0 + \tilde{k} \tilde{W}'_0)}{\chi_0}, \quad \tilde{\phi}(\tilde{r}) = \eta(\xi),$$

$$a = \frac{(\tilde{m}^2 + r_0^2 \tilde{k}^2) \chi_0''}{r_0^2 \chi_0}, \quad \xi = (-2i)^{1/2} \left(a^{1/4} \tilde{r} - \frac{b}{2a^{3/4}} \right). \quad (15)$$

Thus, the inner problem becomes

$$\frac{d^2 \eta}{d\xi^2} + \left[\frac{1}{2i} \left(\frac{b^2}{4a^{3/2}} - \frac{2i(\tilde{m}^2 + r_0^2 \tilde{k}^2)(\tilde{\omega} + \Gamma_0)}{r_0^2 \chi_0 a^{1/2}} \right) - \frac{\xi^2}{4} \right] \eta = 0. \quad (16)$$

Solutions of this equation are Weber-Hermite functions $\eta_n(\xi) = \exp(-\xi^2/4) H_n(\xi)$ [where $H_n(\xi)$ are Hermite polynomials] if the eigenvalues satisfy the following relation:

$$\frac{1}{2i} \left(\frac{b^2}{4a^{3/2}} - \frac{2i(\tilde{m}^2 + r_0^2 \tilde{k}^2)(\tilde{\omega} + \Gamma_0)}{r_0^2 \chi_0 a^{1/2}} \right) = n + \frac{1}{2}, \quad n \in \mathbb{N}, \quad (17)$$

and to satisfy the boundary condition $\phi(r \rightarrow \infty) = 0$, η has to verify the condition $\eta(\xi \rightarrow \infty) = 0$; therefore, $-\pi/4 < \arg(\xi) < \pi/4$.

Finally, we find that for a three-dimensional instability, the complex frequency is given by the following dispersion relation (after simplification and using the original variables):

$$\omega^{(n)} = (m\Omega_0 + kW_0 - \Gamma_0) + i \left[\chi_0 - \left(n + \frac{1}{2} \right) r_0 \sqrt{\frac{-\chi_0'' \chi_0}{m^2 + k^2 r_0^2} + \frac{(kW'_0 + m\Omega'_0)^2}{2\chi_0''}} \right] + O(\varepsilon^{3/2}). \quad (18)$$

Note that when the extremum of χ is a maximum [$\chi_0'' = \chi''(r_0) < 0$], then for all (m, k) , the most unstable eigenmode is the mode $n=0$ (no radial oscillations). Since the terms added to the singular spectrum are corrections, the velocity gradients must scale as

$$(m\Omega'_0 + kW'_0) \sim O(\varepsilon^{1/2}), \quad (19)$$

which is nothing but the scaling $\alpha_3 = 3/2$. Note that when the flow is unstable, the singular spectrum is a superior asymptote for the growth rate. This agrees with the finding of [7] that the points of the singular spectrum are accumulation points for the discrete spectrum.

As a validation, we consider the particular case where $(m\Omega'_0 + kW'_0) = 0$, which is the main assumption used by [6,7]. Then the singular spectrum could be rewritten as

$$\chi^2 = G^2 - 2r\Omega\Omega' \frac{r\Omega'\Theta + W'^2}{W'^2 + r^2\Omega'^2}. \quad (20)$$

Thus, a sufficient condition for the destabilization of the flow is that for some r_0

$$G^2(W'^2 + r^2\Omega'^2) - 2r\Omega\Omega'(r\Omega'\Theta + W'^2) > 0, \quad (21)$$

which is the criterion found by [6].² Note that in the constant-density case, the criterion found by [5] is recovered. The asymptotical results are now checked numerically.

IV. NUMERICAL CHECK

A. Case ($m \neq 0$, $k=0$)

This case could not be described by the analyses of Eckhoff and Storesletten [6], Leibovich and Stewartson [5], and

²However, the modes described by [7] (and [5]) belong to a different branch: their growth rate correction is of order $\varepsilon^{1/2}$; hence, their branch is more amplified.

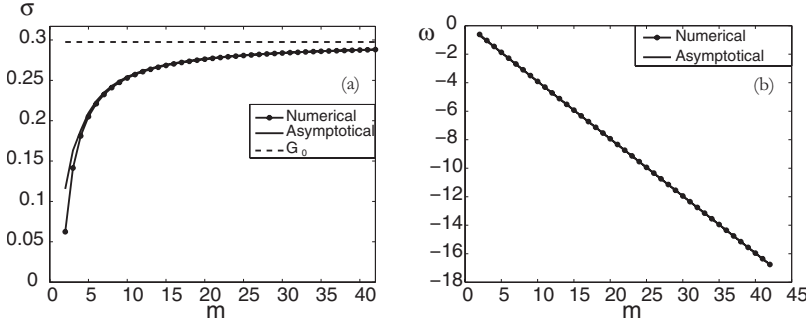


FIG. 1. Comparison between the asymptotic theory and numerical results for $q=-0.4$ and $s=2$, in the ($m \neq 0$, $k=0$) case. (a) The maximum growth rate versus the azimuthal wave number m . Solid line: asymptotics; dotted line: numerics; discontinuous line: the singular spectrum. (b) Real frequency versus m . Solid line: asymptotics (which is also the singular spectrum); dotted line: numerics (the two curves are practically indistinguishable).

Leblanc and LeDuc [7] for nonuniform $\Omega(r)$ and $W(r)$. Non-axisymmetric two-dimensional perturbations are considered. As noted previously, this instability is not affected by the axial velocity. For $k=0$, $\chi^2=G^2$ and the discrete complex frequencies are given by the following dispersion relation:

$$\omega^{(n)} = m\Omega_0 - \Gamma_0 + i \left[G_0 - \left(n + \frac{1}{2} \right) \frac{r_0 \sqrt{-G_0'' G_0}}{m} + \frac{m^2 \Omega_0'^2}{2G_0''} \right] + O(\varepsilon^{3/2}), \quad (22)$$

with $G_0 = \sqrt{G^2(r_0)}$, and r_0 is the location of the extremum of G .

To validate this asymptotic theory, variable-density and incompressible Euler equations are solved numerically. Two kinds of numerical method are used: a shooting method [9], in the complex plane, is used to solve Eq. (6) [with boundary condition $\phi(0) = \phi(\infty) = 0$], and spectrally accurate Chebyshev polynomials are used to solve the eigenvalue problem (1) as described in [3]. The basic flow studied here is a simplified version of the Batchelor q vortex, with density variations. In a cylindrical frame, the velocity field is $\mathbf{U}(\mathbf{x}) = V\mathbf{e}_\theta + W\mathbf{e}_z$, with $V(r) = q\bar{W}[1 - \exp(-r^2/b^2)]/(r/b)$ and $W(r) = \bar{W} \exp(-r^2)$, where \bar{W} is the velocity scale and q is the swirl intensity. The density is an axisymmetric profile, and it is chosen as

$$\rho_b(r) = \rho_\infty [1 + (s-1)\exp(-r^2)], \quad (23)$$

where ρ_∞ is the density at $r=\infty$, and s is the (axial to ambient) density ratio. The core lengths of the axial velocity W and the density ρ_b are chosen equal to 1. According to relation (19), the core length of the azimuthal velocity must be $b \sim O(\varepsilon^{-3/2})$.

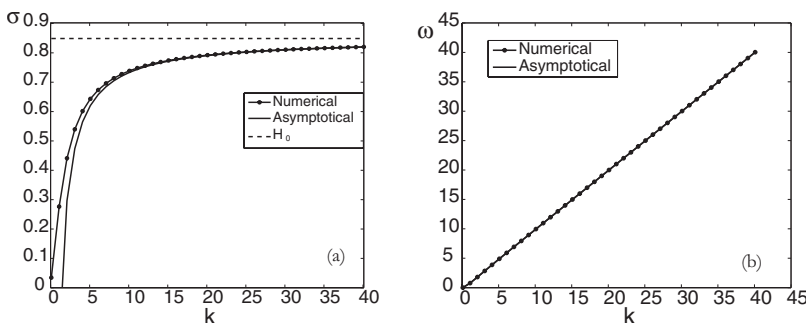


FIG. 2. Comparison between the asymptotic theory and numerical results for $q=-2$ and $s=10$, in the ($m=0$, $k \neq 0$) case. (a) The maximum growth rate versus the axial wave number k . Solid lines: asymptotics; dotted line: numerics; discontinuous line: the singular spectrum. (b) The real frequency versus k . Solid line: asymptotics (which is also the singular spectrum); dotted line: numerics (the two curves are practically indistinguishable).

Figure 1 shows the growth rate and the real frequency versus the azimuthal wave number m for $q=-0.4$ and $s=2$. The two curves (the numerical and the asymptotical) for the real frequency are practically indistinguishable, and those for the growth rate are very close to each other. The error for the growth rate is $<5\%$ for $m > 3$. We have checked numerically that the main features of the singular spectrum and those of the discrete one are preserved when the weakness of angular velocity gradients is relaxed and $b \sim O(1)$ is used, especially that G_0 is a superior asymptote for the growth rate.

B. Case ($m=0$, $k \neq 0$)

This case, also, could not be described by the analyses of Eckhoff and Storesletten [6], Leibovich and Stewartson [5], and Leblanc and LeDuc [7] for nonuniform $\Omega(r)$ and $W(r)$. Here, $\chi^2 = H^2$ and

$$\omega^{(n)} = kW_0 + i \left[H_0 - \left(n + \frac{1}{2} \right) \frac{\sqrt{-H_0'' H_0}}{k} + \frac{k^2 W_0'^2}{2H_0''} \right] + O(\varepsilon^{3/2}), \quad (24)$$

with $H_0 = \sqrt{H^2(r_0)}$. The asymptotic theory is validated by the same numerical procedure as in the previous section, using the basic velocity profile: $V(r) = q\bar{W}[1 - \exp(-r^2)]/r$, $W(r) = \bar{W} \exp(-r^2/b^2)$, and the density profile (23). According to Eq. (19), b is chosen as $b \sim O(\varepsilon^{-3/4})$.

Figure 2 shows the maximum growth rate and the real frequency of the most unstable mode of the asymptotical theory and the numerical results, versus the axial wave number k , for $s=10$ and $q=-2$. The error in the growth rate is $<5\%$ for $k > 4$. We have checked, numerically, that the main

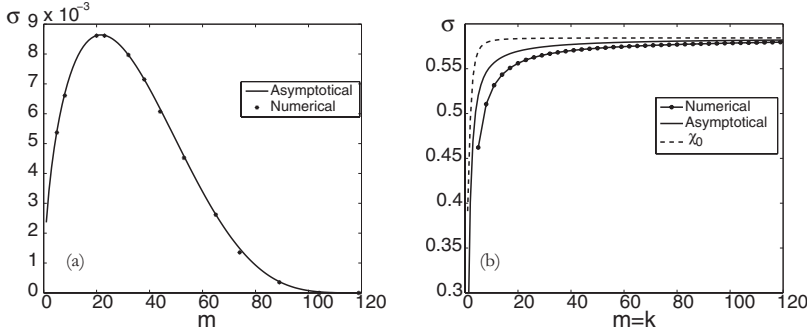


FIG. 3. The maximum growth rate versus the wave number k and/or m . (a) $s=0.5$, $q=-2$, and $k=50$ (note that the asymptotical corrections are very small and cannot be distinguished from the singular spectrum). (b) $s=100$ and $q=-0.4$.

features of the singular spectrum and those of the discrete one are preserved when the weakness of axial velocity gradients is relaxed and $b \sim O(1)$ is used, particularly that H_0 is a superior asymptote for the growth rate.

C. Coupling case

This section is devoted to a mixing of both orthogonal states, especially to their coupling. Therefore, we assume that $k \neq 0$ and $m \neq 0$, and Eq. (6) is considered.

First, the asymptotical theory developed in the general three-dimensional case is validated using similar velocity and density profiles as in the two previous sections. Figure 3 shows the good agreement between numerical results and the asymptotical ones. Two cases are considered. In the first one, $s=0.5$ and $q=-2$, corresponding to a *stable* ($m=0, k \neq 0$) and ($m \neq 0, k=0$) configuration. However, the flow is (weakly) unstable due to the coupling term between azimuthal and axial velocities, i.e., $2kmr\Omega W'/(m^2+k^2r^2)$. The second case is, for example, a case where the term χ^2 is mainly dominated by the ($m \neq 0, k=0$) contribution G^2 ($s=100, q=-0.4$): the error measured for the growth rate is $<5\%$ if $m > 8$ and $k > 8$. We have checked, numerically, that the main features of the singular spectrum and those of the discrete one are preserved when the weakness of velocity gradients is relaxed and $b \sim O(1)$ is used, especially that χ_0 is a superior asymptote for the growth rate.

Second, for a fixed k and $m \rightarrow \infty$ the function $\chi \rightarrow G$, and the instability has the features of the ($m \neq 0, k=0$) case. For, m fixed and $k \rightarrow \infty$ the function $\chi \rightarrow H$, and the instability has the features of the ($m=0, k \neq 0$) case.

Finally, to determine which instability is leading, for the family of variable-density Batchelor-like vortices considered here, isolines of the maximum growth rate (over finite k and m) are plotted in the (q, s) plane, for the three kinds of instabilities using G, H , and χ . This is shown in Fig. 4. These contour plots are obtained using the same core length (equal to 1) for the velocity and density profiles. Clearly, the instability with ($m=0, k \neq 0$) is less unstable. Here, the flow is always stable if $s \leq 3$, whereas in the ($m \neq 0, k=0$) case the flow is always unstable if $s \geq 1$. For the three-dimensional instability, the flow is always stable if $s < 1$ and $q < -5$, whereas it is unstable for all s if $q > -1.8$. This last remark is very important, because it highlights the fact that the coupling between axial and azimuthal velocities destabilizes the flow, even if the vortex is lighter than the ambient fluid. Notice that, for high values of s , the growth rates of the three

instabilities, described above, are independent of the density ratio, whereas this amplification rate grows linearly with the swirl intensity q . Finally, when s and q are high, the growth rate of the three-dimensional instability is very close to the

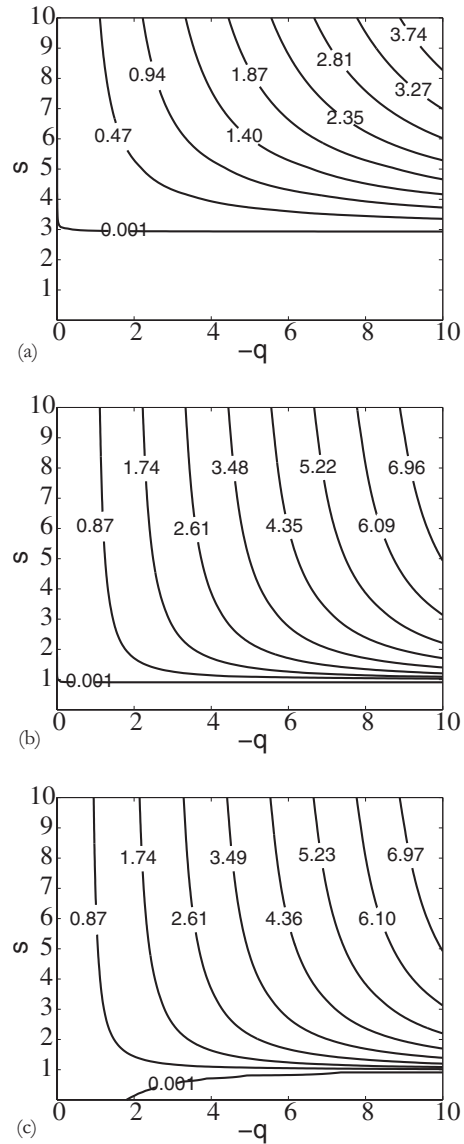


FIG. 4. Isolines of the maximum growth rate ($\forall k, m \in [3, 100]$) in the (q, s) plane, for the (a) ($m=0, k \neq 0$), (b) ($m \neq 0, k=0$), and (c) three-dimensional (generalized) instabilities.

($m \neq 0, k=0$) case, and we conjecture that it leads to a “helical” Rayleigh-Taylor instability.

V. CONCLUSION

Previous asymptotical studies (in the large-wave-number limit) of swirling flows, which break down when $kW'(r)+m\Omega'(r) \neq 0, \forall r$ or if $kW'(r)+m\Omega'(r)=0, \forall r$, are extended to the case $kW'(r)+m\Omega'(r)=O(\beta)$, with β being a small *nonzero* parameter and velocity gradients are assumed weak. We are able to describe instability branches with ($m=0, k \neq 0$) or ($m \neq 0, k=0$), branches that could not be described by the analyses of Eckhoff and Storesletten [6], Leibovich and Stewartson [5], and Leblanc and LeDuc [7] for nonuniform $\Omega(r)$ and $W(r)$. For the three-dimensional instability we show that the asymptotical growth rate could be written as a linear combination of those of the above branches, and this result is summed up in Fig. 5. The asymptotic results are checked using numerically computed growth rates of the linearized Euler equations for a family of variable-density Batchelor-like vortices as base flows. Good agreement is found even for low values of wave numbers m and k . Note that the present analysis is valid for fully compressible flows if the function G^2 is replaced with its fully compressible counterpart ($-N^2$ in [7]) and Γ_0 is given by Eq. (4.3) of the same reference.

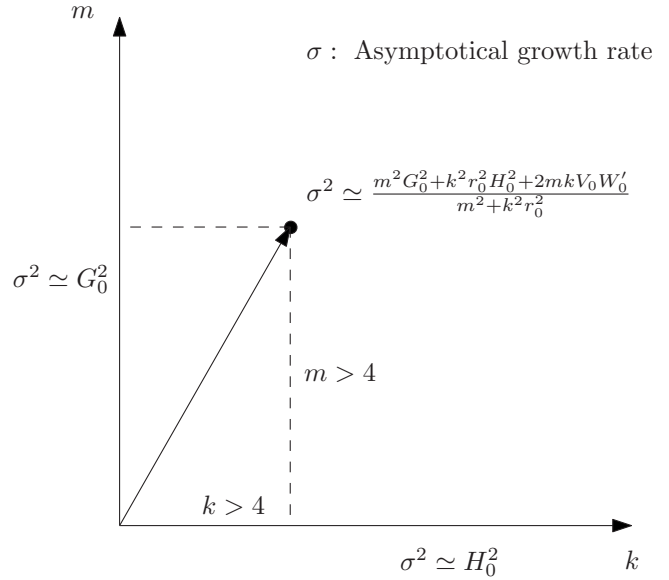


FIG. 5. Asymptotical growth rate σ in the plane (k, m) .

ACKNOWLEDGMENTS

Fruitful discussions with S. Ledizès and E. Villermaux, both of whom kindly read the manuscript, are acknowledged. Fruitful discussions with S. Leblanc are also acknowledged.

[1] M. Abid and M. E. Brachet, *Phys. Fluids* **10**, 469 (1998).
 [2] O. Cadot, S. Douady, and Y. Couder, *Phys. Fluids* **7**, 630 (1995).
 [3] M. Abid, *J. Fluid Mech.* **605**, 19 (2008).
 [4] L. N. Howard and A. S. Gupta, *J. Fluid Mech.* **14**, 463 (1962).
 [5] S. Leibovich and K. Stewartson, *J. Fluid Mech.* **126**, 335 (1983).

[6] K. S. Eckhoff and L. Storesletten, *J. Fluid Mech.* **89**, 401 (1978).
 [7] S. Leblanc and A. LeDuc, *J. Fluid Mech.* **537**, 433 (2005).
 [8] D. Sipp, D. Fabre, S. Michelin, and L. Jacquin, *J. Fluid Mech.* **526**, 67 (2005).
 [9] M. Abid, M. E. Brachet, and P. Huerre, *Eur. J. Mech. B/Fluids* **12**(5), 683 (1993).